Supporting Information

Engineering of Thiocyanate-free Ru(II) Sensitizers for High Efficiency Dye-Sensitized Solar Cells

Sheng-Wei Wang[a], Kuan-Lin Wu[a,b], Elham Ghadiri[b], Maria Grazia Lobello[c], Shu-Te Ho[a], Yun Chi*[,a], Jacques-E. Moser*[,b], Filippo De Angelis*[,c], Michael Grätzel[b], Mohammad K. Nazeeruddin[*,b]

S.-W.W. and K.-L.W. contributed equally to this work.

[a] Department of Chemistry and Low Carbon Energy Research Center, National Tsing Hua University, Hsinchu 30013, Taiwan; E-mail: ychi@mx.nthu.edu.tw

[b] Laboratory of Photonics and Interfaces, Institute of Chemical Sciences and Engineering, Ecole Polytechnique Fédérale de Lausanne (EPFL), CH-1015 Lausanne, Switzerland; E-mail: mdkhaja.nazeeruddin@epfl.ch

[c] Computational Laboratory for Hybrid/Organic Photovoltaics (CLHYO), ISTM-CNR, Via Elce di Sotto 8, 06123, Perugia, Italy; E-mail: filippo@thch.unipg.it

Synthetic Experiments

General procedures: All reactions were performed under argon atmosphere and solvents were distilled from appropriate drying agents prior to use. Commercially available reagents were used without further purification unless otherwise stated. All reactions were monitored using pre-coated TLC plates (0.20 mm with fluorescent indicator UV254). Mass spectra were obtained on a JEOL SX-102A instrument operating in electron impact (EI) or fast atom bombardment (FAB) mode. ^{1}H NMR spectra were recorded on a Varian Mercury-400 or an INOVA-500 instrument.

Elemental analysis was carried out with a Heraeus CHN-O Rapid Elementary Analyzer.

Synthesis of 1-(4-(5-(hexylthio)thiophen-2-yl)pyridin-2-yl)ethanone. 2-Acetyl-4-chloropyridine (1.03 g, 6.62 mmol), 2-(5-(hexylthio)thiophen-2-yl)-4,4,5,5-tetramethyl-1,3,2-dioxaborolane (2.53 g, 7.75 mmol), $Pd(PPh_3)_4$ (0.372 g, 3.20 mmol), and aqueous Na_2CO_3 (2.1 g, 19.4 mmol) were dissolved in a mixture of THF (60 mL). The mixture was refluxed for 15 h. After then, the solvent was removed under reduced pressure, and the residue was extracted with ethyl acetate (2 × 100 mL), dried over $MgSO_4$ and evaporated to dryness. The pure product was further purified by column chromatography with hexane/ ethyl acetate = 4/1 as eluent, giving 1.61 g of viscous yellow oil (65%).

Selected spectral data: ^{1}H NMR (400 MHz, $CDCl_3$, 298 K): δ 8.61 (dd, *J* = 0.40, 5.2 Hz, 1H), 8.13 (dd, *J* = 0.40, 1.8 Hz, 1H), 7.54 (dd, *J* = 2.0, 5.2 Hz, 1H), 7.43 (d, *J* = 3.6, 1H), 7.07 (d, *J* = 3.6 Hz, 1H), 2.87 (t, *J* = 7.2 Hz, 2H), 2.73 (s, 3H), 1.68 ~ 1.60 (m, 2H), 1.43 ~ 1.26 (m, 6H), 0.85 (t, *J* = 5.0 Hz, 3H).

Synthesis of 4-(5-(hexylthio)thiophen-2-yl)-2-(3-(trifluoromethyl)-1H-pyrazol-5-yl)pyridine. To a stirred suspension of NaOEt (0.550 g, 8.08 mmol) in 40 mL of THF was added a 30 mL THF solution of 1-(4-(5-(hexylthio)thiophen-2-yl) pyridin-2-yl)ethanone (1.72 g, 5.38 mmol) and ethyl trifluoroacetate (0.833 mL, 6.12 mmol). The mixture was refluxed for 12 h and, after cooling, the solution was neutralized with 2 M HCl until pH 5−6. THF solvent was removed and the residue was extracted with CH_2Cl_2 (3 × 80 mL). The combined extract was washed with water, dried over anhydrous $MgSO_4$, and concentrated under vacuum to give the corresponding β-diketone. Without further purification, hydrazine monohydrate (98%, 1.3 mL, 28 mmol) was added into the abovementioned β-diketone dissolved in EtOH (50 mL). The mixture was refluxed for 12 h and the solvent was evaporated.

Finally, after the removal of excess of hydrazine, the product was purified by silica gel column chromatography (hexane/ethyl acetate = 3:1) to give yellow solid (1.37 g, 62%).

Selected spectral data: MS (EI), m/z 411 $(M)^+$. ^{1}H NMR (400 MHz, $CDCl_3$, 298 K): δ 12.02 (s, 1H), 8.55 (d, *J* = 5.2 Hz, 1H), 7.72 (s, 1H), 7.44 (m, 2H), 7.10(d, *J* = 4.0 Hz, 1H), 7.04 (s, 1H), 2.90 (t, *J* = 7.2 Hz, 2H), 1.70 ~ 1.62 (m, 2H), 1.43 ~ 1.27 (m, 6H), 0.87 (t, *J* = 6.9 Hz, 3H).

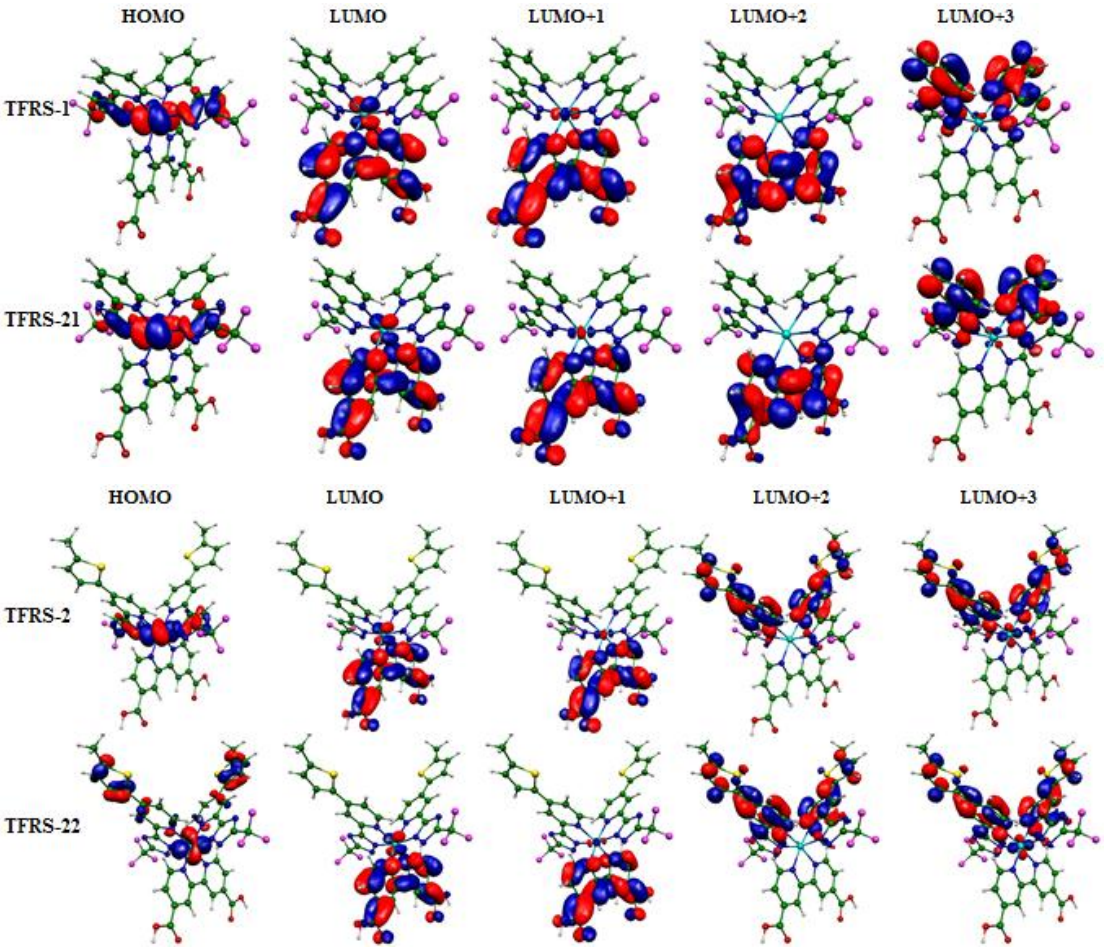

Figure S1. Isodensity plot (isodensity value 0.035) of the HOMO and of various LUMOs of **TFRS-1** and **-21**, and **TFRS-2** and **-22**.

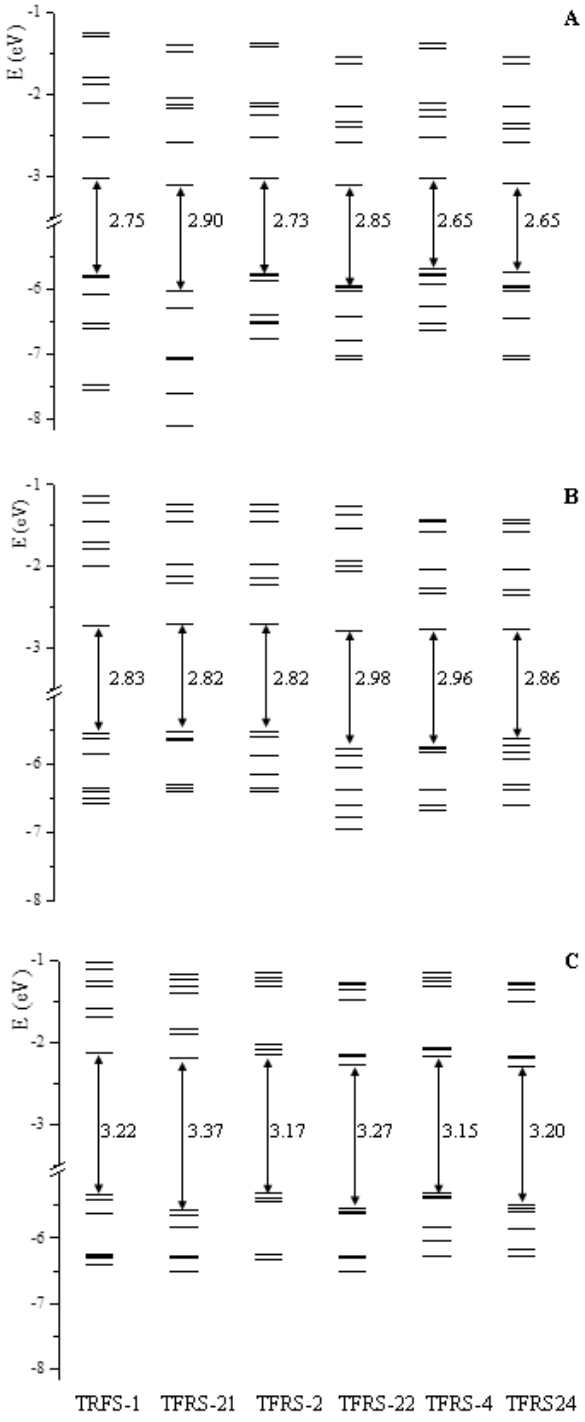

Figure S2. Schematic representation of the energy levels of the neutral doubly protonated, A, mono protonated, B, and doubly deprotonated, C, **TFRS-1**, **-21**, **-2**, **-22**, **-4** and **-24** complexes.

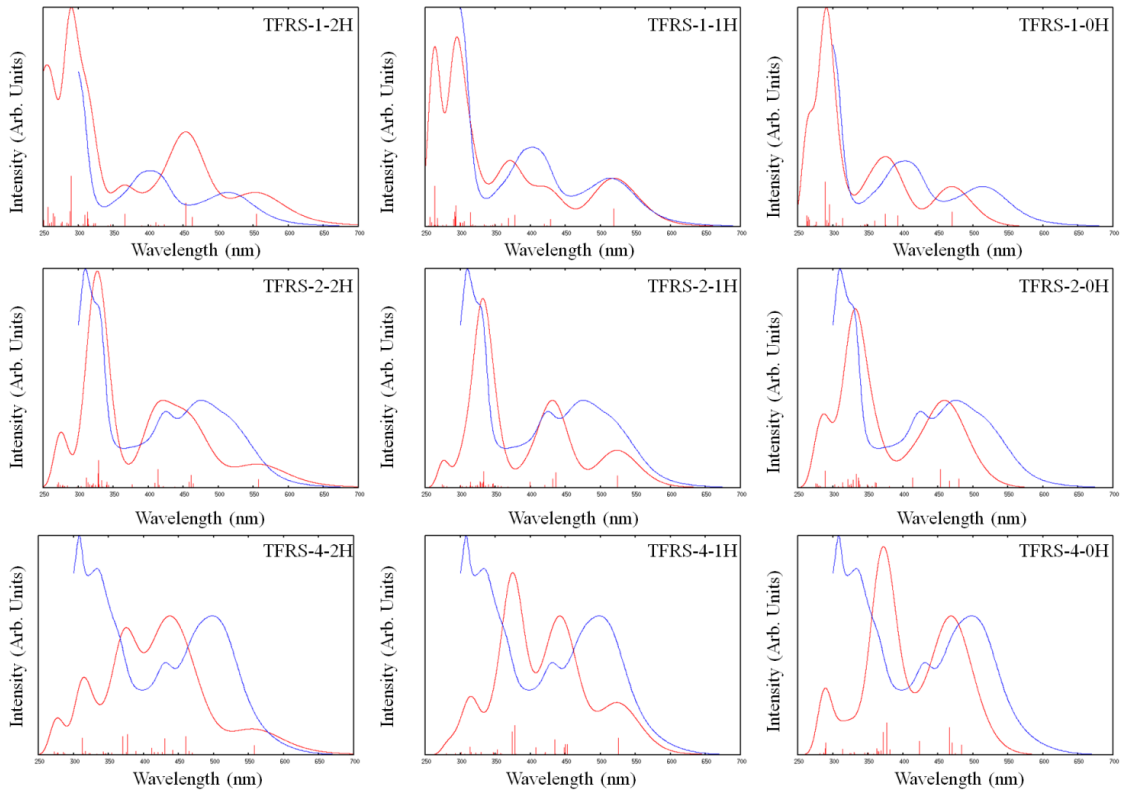

Figure S3. Comparison between the experimental (blue lines) and calculated (red lines) (doubly protonated, left, mono protonated, center, doubly deprotonated right) optical absorption spectra for the TFRS-1/-4 series. The intensity of the experimental spectra have been rescaled to match those of the computed visible maximum. Vertical lines correspond to unbroadened oscillator strengths.

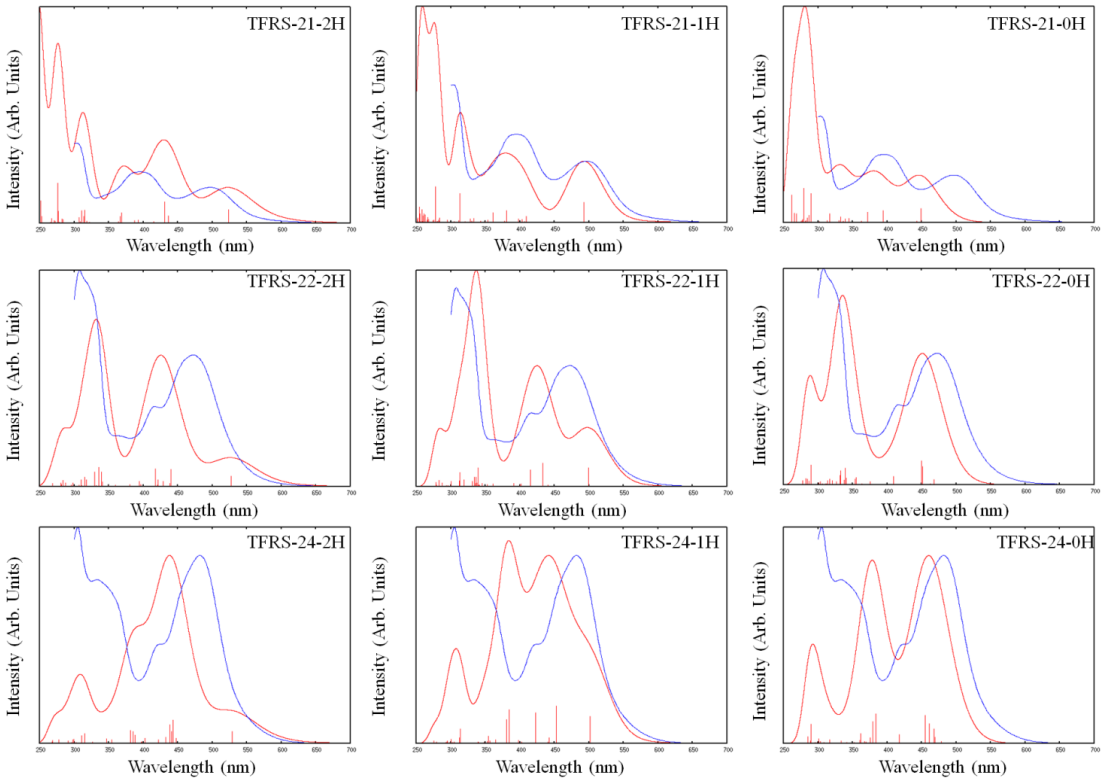

Figure S4. Comparison between the experimental (blue lines) and calculated (red lines) (doubly protonated, left, mono protonated, center, doubly deprotonated right) optical absorption spectra for the TFRS-21/-24 series. The intensity of the experimental spectra have been rescaled to match those of the computed visible maximum. Vertical lines correspond to unbroadened oscillator strengths.

Table S1. Energies of the lowest unoccupied and highest occupied Kohn-Sham orbitals of **TFRS-1/-2/-4** doubly protonated (**2H**), mono protonated, (**1H**) and doubly deprotonated (**0H**). Energy in eV.

	TFRS-1			**TFRS-2**			**TFRS-4**		
	2H	**1H**	**0H**	**2H**	**1H**	**0H**	**2H**	**1H**	**0H**
H-6	-7.54	-6.57	-6.40	-6.76	-6.41	-6.32	-6.64	-6.40	-6.27
H-5	-7.46	-6.50	-6.31	-6.51	-6.40	-6.26	-6.51	-6.35	-6.27
H-4	-6.61	-6.41	-6.27	-6.50	-6.35	-6.26	-6.26	-6.14	-6.04
H-3	-6.51	-6.35	-6.26	-6.38	-6.30	-6.25	-5.92	-5.86	-5.82
H-2	-6.06	-5.84	-5.62	-5.85	-5.64	-5.45	-5.78	-5.60	-5.38
H-1	-5.80	-5.63	-5.40	-5.79	-5.61	-5.39	-5.77	-5.53	-5.37
H	-5.78	-5.55	-5.34	-5.75	-5.53	-5.32	-5.67	-5.52	-5.32
L	-3.03	-2.72	-2.12	-3.02	-2.71	-2.15	-3.02	-2.71	-2.17
L+1	-2.52	-1.99	-1.69	-2.52	-2.20	-2.08	-2.52	-2.23	-2.09
L+2	-2.10	-1.78	-1.59	-2.24	-2.12	-2.03	-2.27	-2.15	-2.07
L+3	-1.88	-1.69	-1.31	-2.14	-1.97	-1.32	-2.18	-1.97	-1.32
L+4	-1.79	-1.46	-1.25	-2.09	-1.46	-1.25	-2.09	-1.45	-1.25
L+5	-1.29	-1.22	-1.11	-1.41	-1.32	-1.21	-1.42	-1.32	-1.21
L+6	-1.24	-1.13	-1.03	-1.37	-1.25	-1.15	-1.37	-1.25	-1.16

Table S2. Energies of the lowest unoccupied and highest occupied Kohn-Sham orbitals of **TFRS-21/-22/-24** doubly protonated (**2H**), mono protonated, (**1H**) and doubly deprotonated (**0H**). Energy in eV.

	TFRS-21			**TFRS-22**			**TFRS-24**		
	2H	**1H**	**0H**	**2H**	**1H**	**0H**	**2H**	**1H**	**0H**
H-6	-8.11	-6.94	-6.52	-7.07	-6.68	-6.50	-7.07	-6.59	-6.29
H-5	-7.59	-6.77	-6.51	-7.03	-6.59	-6.31	-7.03	-6.38	-6.28
H-4	-7.08	-6.60	-6.30	-6.78	-6.37	-6.29	-6.44	-6.29	-6.17
H-3	-7.04	-6.38	-6.29	-6.42	-6.36	-6.28	-6.02	-5.91	-5.86
H-2	-6.27	-6.05	-5.84	-6.01	-5.82	-5.61	-5.97	-5.81	-5.60
H-1	-6.03	-5.86	-5.64	-5.98	-5.78	-5.60	-5.93	-5.73	-5.54
H	-6.01	-5.77	-5.57	-5.95	-5.74	-5.54	-5.74	-5.63	-5.49
L	-3.11	-2.79	-2.20	-3.10	-2.78	-2.27	-3.09	-2.77	-2.29
L+1	-2.58	-2.05	-1.91	-2.57	-2.33	-2.17	-2.57	-2.35	-2.20
L+2	-2.17	-2.00	-1.83	-2.40	-2.26	-2.16	-2.42	-2.28	-2.17
L+3	-2.11	-1.93	-1.41	-2.32	-2.03	-1.49	-2.35	-2.03	-1.50
L+4	-2.03	-1.54	-1.32	-2.15	-1.57	-1.37	-2.15	-1.57	-1.37
L+5	-1.47	-1.37	-1.24	-1.61	-1.46	-1.29	-1.61	-1.47	-1.29
L+6	-1.38	-1.27	-1.17	-1.53	-1.42	-1.27	-1.53	-1.43	-1.27

Table S3. Computed excitation energies (eV and nm) and oscillator strengths (*f*) for the optical transitions of TFRS-1 in aqueous solution.

	N_state	E (eV)	WL (nm)	f	Composition (%)	
TFRS-1_2H	3	2.24	554	0.1201	H-1 → L	84
	4	2.68	463	0.0912	H-1 → L+1	97
	5	2.73	454	0.2287	H → L+1	79
	7	2.94	422	0.0227	H-3 → L+1	93
	8	2.99	415	0.0135	H → L+2	93
	10	3.02	410	0.0393	H-1 → L+2	90
	11	3.07	403	0.0170	H → L+3	93
	13	3.18	390	0.0126	H-1 → L+4	94
TFRS-1_1H	3	2.39	519	0.1907	H-1 → L	91
	4	2.89	429	0.0804	H → L+1	77
	5	2.93	423	0.0136	H → L+2	87
	6	2.95	420	0.0287	H-1 → L+1	74
	7	2.96	419	0.0173	H-1 → L+1 H → L+3	20 62
	14	3.28	378	0.1218	H-2 → L+2	88
TFRS-1_0H	3	2.64	470	0.1679	H-1 → L	93
	8	3.16	393	0.1273	H-2 → L+1	91
	9	3.31	375	0.0173	H → L+3	96
	10	3.31	374	0.1415	H-2 → L+2 H → L+4	51 36
	14	3.45	360	0.0678	H-1 → L+5	94

Table S4. Computed excitation energies (eV and nm) and oscillator strengths (*f*) for the optical transitions of TFRS-2 in aqueous solution.

	N_state	E (eV)	WL (nm)	f	Composition (%)	
TFRS-2_2H	3	2.22	558	0.1656	H-1 → L	84
	4	2.67	464	0.0851	H-1 → L+1	97
	5	2.69	461	0.2376	H-2 → L+1	21
					H → L+1	65
	6	2.71	458	0.1126	H-2 → L+1	73
	7	2.83	438	0.0201	H → L+2	92
	11	2.94	421	0.0290	H-5 → L	77
	13	2.99	415	0.0481	H-2 → L+2	34
					H → L+4	58
	14	3.00	414	0.3477	H-2 → L+2	53
					H → L+4	35
TFRS-2_1H	3	2.37	524	0.2756	H-1 → L	87
	8	2.84	436	0.3498	H-2 → L+1	88
	9	2.87	432	0.2063	H → L+3	81
	10	2.95	421	0.0634	H-1 → L+3	95
	11	3.00	414	0.0156	H-2 → L+3	90
	12	3.10	400	0.1286	H-2 → L+2	51
	14	3.17	391	0.0173	H-6 → L	55
TFRS-2_0H	5	2.58	480	0.1729	H-1 → L	95
	7	2.66	466	0.1293	H-1 → L+1	83
	8	2.73	453	0.3604	H-2 → L	46
					H-2 → L+1	45
	9	3.00	414	0.1975	H-2 → L+2	72
					H → L+4	10
	10	3.26	381	0.0358	H → L+3	96
	12	3.39	366	0.0106	H → L+5	84
	14	3.43	362	0.0959	H-1 → L+4	88

Table S5. Computed excitation energies (eV and nm) and oscillator strengths (*f*) for the optical transitions of TFRS-4 in aqueous solution.

	N_state	E (eV)	WL (nm)	f	Composition (%)	
TFRS-4_2H	3	2.22	558	0.1878	H-2 → L	83
	4	2.59	480	0.0129	H-3 → L	87
	5	2.64	470	0.0470	H → L+1	78
	6	2.67	465	0.0791	H-2 → L+1	96
	7	2.69	460	0.3656	H-1 → L+1	77
	8	2.74	453	0.0138	H-4 → L	81
	9	2.81	441	0.0965	H-1 → L+2	67
					H → L+1	30
	10	2.86	434	0.0162	H-1 → L+3	73
	11	2.88	431	0.3214	H-2 → L+2	19
					H-1 → L+1	21
					H → L+2	47
	12	2.88	431	0.1085	H-2 → L+2	54
	13	2.91	426	0.0549	H-2 → L+3	95
	14	2.95	421	0.0490	H-5 → L	92
	15	2.99	415	0.0526	H-1 → L+4	71
					H → L+4	26
TFRS-4_1H	3	2.36	525	0.3165	H-2 → L	89
	6	2.74	453	0.2012	H-2 → L+1	29
					H-1 → L+1	36
	7	2.75	450	0.2002	H-2 → L+1	61
					H-1 → L+1	23
	8	2.77	448	0.1360	H-2 → L+2	84
	9	2.85	435	0.0228	H-3 → L	92
	10	2.85	435	0.2935	H-1 → L+3	23
					H → L+3	46
	11	2.94	422	0.0474	H-2 → L+3	86
	12	2.95	420	0.0219	H-1 → L+3	58
	14	3.04	408	0.1408	H-1 → L+2	31
					H → L+3	23
TFRS-4_0H	5	2.56	484	0.1766	H-2 → L	93
	6	2.61	475	0.0243	H-2 → L+2	77
	7	2.64	470	0.2130	H-2 → L+1	74

	8	2.67	467	0.4746	H-2 → L+2 H-1 → L H-1 → L+1	16 55 26
	9	2.93	423	0.2377	H-2 → L+1 H-1 → L+2	14 71
	10	3.25	382	0.0892	H → L+3	92
	11	3.29	377	0.5571	H-3 → L	89
	12	3.33	372	0.3986	H-4 → L H-3 → L+2	20 53
	14	3.37	368	0.0709	H-1 → L+3 H → L+5	63 13
	15	3.39	366	0.0521	H → L+5	78

Table S6. Computed excitation energies (eV and nm) and oscillator strengths (*f*) for the optical transitions of TFRS-21 in aqueous solution.

	N_state	E (eV)	WL (nm)	f	Composition (%)	
TFRS-21_2H	3	2.37	523	0.1993	H-1 → L	87
	4	2.84	436	0.0789	H-1 → L+1	97
	5	2.88	431	0.2252	H → L+1	82
	6	2.99	415	0.0166	H-2 → L+1	94
	11	3.16	393	0.0309	H-1 → L+4	65
	12	3.20	387	0.0251	H-1 → L+2	67
	13	3.36	369	0.1085	H-2 → L+3	85
	14	3.38	367	0.0682	H-3 → L	86
TFRS-21_1H	3	2.52	493	0.1975	H-1 → L	90
	6	3.03	409	0.0612	H-1 → L+2	41
					H → L+1	49
	9	3.07	403	0.0285	H-1 → L+2	44
					H → L+1	29
	10	3.12	398	0.0336	H-1 → L+1	87
	12	3.26	381	0.1190	H-2 → L+1	23
					H-2 → L+2	66
	13	3.28	378	0.0131	H-2 → L+1	73
	14	3.43	361	0.0971	H-2 → L+3	48
					H → L+5	35
	15	3.51	354	0.0269	H-5 → L	86
TFRS-21_0H	2	2.76	449	0.1516	H-1 →L	72
					H → L+2	16
	3	2.76	449	0.0121	H-2 → L	86
	5	2.80	443	0.0154	H-1 → L	13
					H→ L+2	78
	8	3.14	394	0.1271	H-2 →L+1	90
	9	3.34	371	0.1117	H-2 → L+2	65
					H → L+4	18
	12	3.42	363	0.0173	H → L+3	98

Table S7. Computed excitation energies (eV and nm) and oscillator strengths (*f*) for the optical transitions of TFRS-22 in aqueous solution.

	N_state	E (eV)	WL (nm)	f	Composition (%)	
TFRS-22_2H	3	2.35	527	0.2019	H-2 → L	86
	5	2.82	440	0.3197	H-1 → L+1	60
	6	2.83	439	0.0593	H-2 → L+1	96
	7	2.87	432	0.0126	H-1 → L+2	88
	8	2.89	429	0.0989	H-1 → L+3	78
	9	2.94	421	0.1279	H-2 → L+3	38
					H → L+2	49
	10	2.95	420	0.0255	H-2 → L+2	80
	11	2.97	418	0.3366	H-2 → L+3	57
					H → L+2	38
	13	3.13	396	0.0351	H-1 → L+4	88
	14	3.15	394	0.0943	H-2 → L+4	72
					H → L+3	23
TFRS-22_1H	3	2.48	500	0.3115	H-2 → L	89
	6	2.81	441	0.0284	H-2 → L+1	25
					H-1 → L+2	36
					H-1 → L+1	28
	8	2.86	434	0.3918	H-1 → L+1	68
	9	2.99	415	0.2755	H-1 → L+2	29
					H → L+3	66
	11	3.09	402	0.0415	H-2 → L+3	84
	12	3.10	400	0.0272	H-1 → L+3	76
	13	3.17	391	0.0549	H-1 → L+2	32
					H → L+3	18
TFRS-22_0H	5	2.65	468	0.0887	H-1 → L	97
	6	2.68	463	0.0135	H-2 → L	24
					H-1 → L+1	70
	7	2.75	451	0.2988	H-2 → L+2	23
					H-1 → L+2	74
	8	2.76	450	0.3936	H-2 → L	59
					H-2 → L+2	25
					H-1 → L+1	12
	9	3.03	409	0.1408	H-2 → L+1	64

					H-1 → L+2	19
	10	3.30	375	0.0503	H → L+3	97
	14	3.41	363	0.0148	H → L+3	94
	15	3.49	355	0.1177	H-1 → L+3	15
					H → L+4	48
					H-1 → L+6	21

Table S8. Computed excitation energies (eV and nm) and oscillator strengths (*f*) for the optical transitions of TFRS-24 in aqueous solution.

	N_state	E (eV)	WL (nm)	f	Composition (%)	
TFRS-24_2H	3	2.34	529	0.2345	H-3 → L	62
	5	2.69	460	0.0152	H → L+1	88
	6	2.77	448	0.1033	H-4 → L	67
	7	2.80	443	0.4674	H-2 → L+1	70
	8	2.81	441	0.2346	H → L+2	54
	9	2.83	439	0.3755	H-3 → L+1	52
	11	2.87	433	0.1213	H-2 → L+3	79
	13	2.94	422	0.0729	H-3 → L+3	65
	14	3.08	402	0.0999	H-3 → L+4	21
					H → L+3	43
TFRS-24_1H	3	2.47	501	0.3726	H-2 → L	83
	6	2.74	453	0.5177	H → L+1	83
	7	2.80	443	0.0813	H-2 → L+1	55
	8	2.81	441	0.0239	H-2 → L+2	65
	10	2.93	423	0.4283	H-1 → L+3	37
					H → L+2	47
	14	3.08	403	0.0200	H-2 → L+3	57
	15	3.12	398	0.0461	H-2 → L+3	30
					H-1 → L+3	27
TFRS-24_0H	4	2.59	479	0.0349	H-1 → L	22
					H → L	16
					H → L+2	42
	5	2.64	470	0.0983	H-2 → L	96
	6	2.65	468	0.228	H-2 → L+1	34
					H-1 → L	14
					H → L	43
	7	2.69	461	0.3130	H-2 → L+1	54
					H → L	13
					H → L+2	14
	8	2.72	455	0.4395	H-2 → L+2	62
					H → L+1	28
	9	2.97	418	0.1373	H-2 → L+1	29
					H-2 → L+1	14

					H → L+1	43
	10	3.23	384	0.4662	H-3 → L	96
	11	3.27	380	0.3468	H-3 → L+1	37
					H-2 → L+3	32
					H → L+3	24
	12	3.30	376	0.0939	H-3 → L+1	57
					H-2 → L+3	18
					H → L+3	22
	13	3.36	369	0.0212	H-2 → L+3	47
					H → L+3	44
	14	3.38	367	0.0334	H-3 → L+2	87